21.7 3-D Integrable Optoelectronic Devices for Telecommunications ICs

Paolo Dainesi, Adrian M. Ionescu, Luc Thévenaz, Kaustav Banerjee[1], Michel J. Declercq, Philippe Robert, Philippe Renaud, Philippe Fluckiger, Cyrille Hibert, Georges A. Racine

Swiss Federal Institute of Technology Lausanne (EPFL), Switzerland
[1]Center for Integrated Systems, Stanford University, CA

The 3-D IC architecture has emerged as a potential solution to alleviate the interconnect delay problem in future VLSI and to realize large mixed-signal systems-on-a-chip (SoC) [1]. In particular, heterogeneous integration of photonic circuits using 3-D ICs, e.g., with a microprocessor, to improve performance in large synchronous designs, has attracted major interest. This work deals with the design, fabrication and characterization of some basic CMOS-compatible optoelectronic devices: 2x2 switches and both balanced and unbalanced Mach-Zehnder (MZ) interferometers with and without multi-mode interference (MMI) couplers. All the devices are fabricated on SOI substrates, which makes them particularly suitable for 3-D telecommunication photonic ICs. 5MHz bandwidth is demonstrated for the 2x2 switch and a thermal compensation principle is reported for the modulators.

The use of photonic devices and interconnects in electronic systems suggests mixed multisignal systems with integrated analog, digital, RF, and optical systems. Integrated optoelectronics answers the demands on cost reduction while meeting the performance goals. Employing optical interconnects for global signaling or clocking could eliminate or alleviate many problems associated with large multi-GHz synchronous designs including power dissipation, high I/O pin count, electromagnetic interference and clock skew [1]. Additionally, performance of both photodetectors and receivers is known to be sufficiently immune from increase of noise with temperature, which makes them attractive for 3-D telecommunication ICs.

The proposed optoelectronic devices are fabricated on SOI, which is a unique candidate for 3-D integration due to ease of wafer stacking and reduced length of vertical wires that realize wafer-to-wafer connections. Moreover, SOI provides versatile solutions because of its strong confinement of optical modes (high refractive index difference between air, silicon and SiO_2) and 0.3dB/cm loss. Various works confirm that the most effective mechanism for varying the refractive index of light in pure silicon is the charge injection (or plasma dispersion) effect [2,3,4]. Franz-Keldysh and Kerr effects in silicon are too weak to guarantee reliable applications. Another useful reported mechanism is the thermo-optic effect that is appropriate for refractive index modulation related to slow applications (limited to few 100kHz) [3]. Figure 21.7.1 depicts a typical application of the optoelectronic switch developed in this work: a programmable optical add-drop multiplexer for wavelength division multiplexing (WDM) optical telecommunication networks. Figure 21.7.2 shows another optoelectronic device, the unbalanced MZ interferometer that addresses the filtering of telecommunication signals, e.g., when the selection of a modulating frequency in dual frequency networks or of incoming signal packets is requested. A similar architecture, a symmetrical MZ interferometer, is also realized and used as a test vehicle. Figure 21.7.3 shows 3-D IC architectures using the SOI optoelectronic devices in the second layer and the control electronics in the first layer.

The optoelectronic devices are fabricated on SIMOX substrates on top of which a 10μm-thick Si epi-layer is deposited. 80 PIN diodes per device arm, in parallel configuration, are integrated on top of the SOI rib using standard steps of a low-cost 1.2μm-CMOS process with 2-metal levels. A full diode arm is able to provide around 100mA current with <2.5V applied. The SOI waveguide rib including the diodes, with 10μm width and 4μm height, are defined in a post-processing step by a non-pulsed, room temperature dry etching technique using a SF_6/C_4F_8 gas mixture. Absorption losses are found as low as 1.4dB/cm, mostly due to residual etching roughness of the rib sidewalls. Extinction ratio and crosstalk are about 10dB. The coupling efficiency with a standard optical fiber is >90%.

The device optimization is performed by 2-D numerical device simulation in static and transient regimes, in terms of geometrical dimensions (PIN diode width=10μm and length=8μm) and doping level ($N_A=10^{15}cm^{-3}$). Additionally, simulations reveal that the switching behavior is sensitive to the value of the silicon film carrier lifetime.

The 2x2 optical switch is implemented using the principle of a generalized MZ interferometer with a MMI coupler used for light separation and recombination at the input and output ports. Typical results are shown in Figure 21.7.4. The 5MHz bandwidth measured on this device, together with its pulse format and bit rate transparency, makes it a more attractive candidate for fast switching in WDM optical networks compared to MEMS solutions for which the switching time is limited to 0.1-1ms [5].

The unbalanced MZ interferometer reported in Figure 21.7.2 is conceived as a basic filtering device on the principle that different wavelengths correspond to different phase shifts ($\Delta\phi$) in the two asymmetric device arms. By optimal design of the arm lengths and their separation, passive filtering conditions can be set up: $\Delta\phi(\lambda_1)=2N\pi$ and $\Delta\phi(\lambda_2)=(2N+1)\pi$, where N is an integer. When a refractive index modulation is enabled, filtering becomes active following an additional π phase shift to reverse the previous condition. The total injected power for a shift of π is 450mW. Signals at 1300nm and 1550nm wavelengths are efficiently filtered, (Figure 21.7.5), for modulation frequencies >1MHz.

For lower modulation frequencies (100kHz-800kHz), to overcome the negative impact of the thermo-optic effect, a thermal compensation procedure is introduced (Figure 21.7.6). The thermal compensation could be particularly useful for the 3-D integration scheme, where inhomogeneous thermal effects due to higher temperature rise in the upper layers could be a concern [6]. The idea is simple yet efficient. The phase of the propagating signal is differently modulated in the two MZ arms: in one arm by the plasma effect; in the opposite arm by pure thermal effect that compensates the parasitic thermal effect of the first arm. The PIN diodes of the arm that compensate for thermal effect are operated near breakdown with a reverse bias voltage, (~9V), and a lower current, resulting in same thermal power as the opposite arm. A tunable series resistance is employed for power balance. This principle is generally useful in the 100kHz-1MHz range, where neither of the two modulating effects (plasma and thermal) is dominant.

A die micrograph with the SOI optoelectronic devices, the 2x2 switch and the MZ filtering device, is provided in Figure 21.7.7.

References:

[1] K. Banerjee et al., "3-D ICs: A novel chip design for improving deep submicrometer interconnect performance and systems-on-chip integration," Proc. of the IEEE, vol. 89, no. 5, pp. 602-633, 2001.
[2] R.A. Soref, B.R. Bennett, "Electrooptical effects in silicon", IEEE Journal of Quantum Electron., vol. QE-23, pp. 123-129, 1987.
[3] C. Z. Zhao et al., "Silicon raised strip waveguide based on silicon and silicon dioxide thermal bonding", IEEE Photonics Techn. Let., vol. 9, pp. 473-474, 1997.
[4] P. Dainesi et al., "CMOS compatible fully integrated Mach-Zehnder interferometer in SOI technology", IEEE Photonics Techn. Let., vol. 12, pp. 660-662, 2000.
[5] R.T. Chen et al., "A high-speed low-voltage stress-induced micromachined 2x2 optical switch", IEEE Photonics Techn. Let., vol. 11, pp. 1396-1398, 1999.
[6] A. H. Ajami et al., "Effects of non-uniform substrate temperature on the clock signal integrity in high performance designs," IEEE Custom IC Conf. 2001, pp. 233-236.

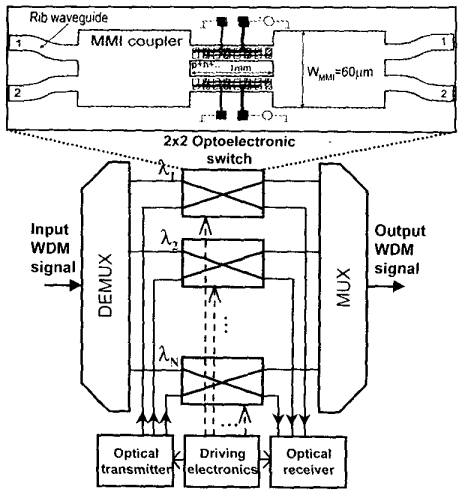

Figure 21.7.1: Optical add-drop multiplexer for WDM optical telecommunications.

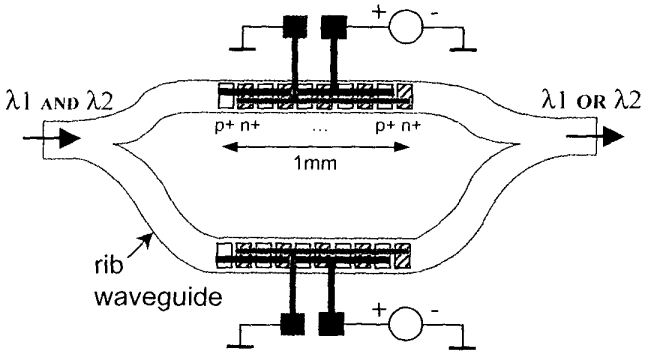

Figure 21.7.2: Unbalanced Mach-Zehnder filtering device.

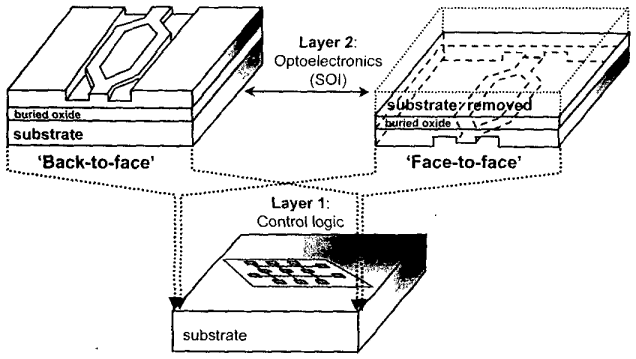

Figure 21.7.3: 3-D integration of SOI optoelectronic devices.

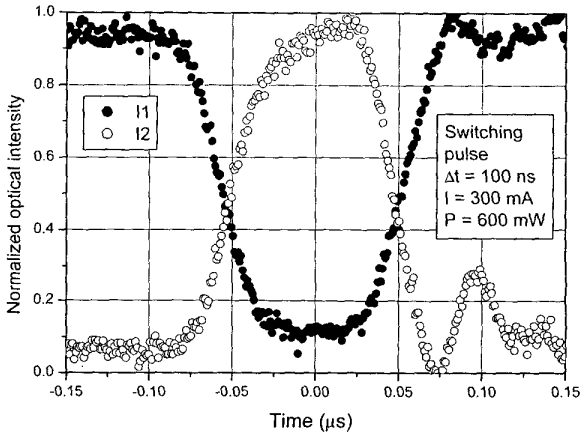

Figure 21.7.4: Normalized optical intensities at the output of the 2x2 optoelectronic switch (λ=1.55μm).

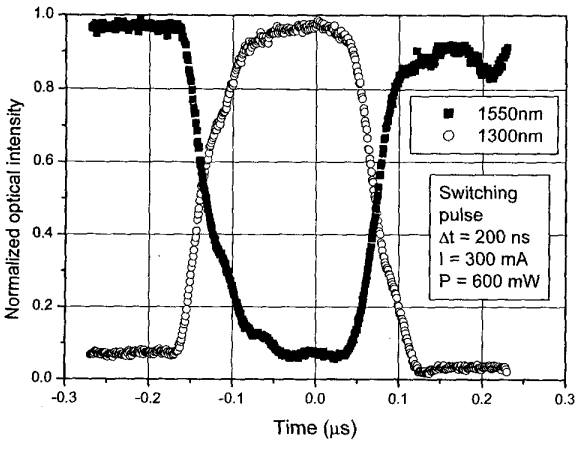

Figure 21.7.5: Normalized optical intensity at the output of the unbalanced MZ device.

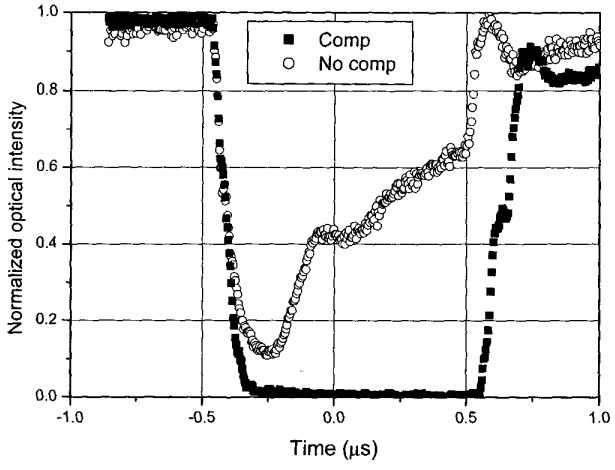

Figure 21.7.6: Normalized optical intensity with and without thermal compensation.

Continued on Page 473

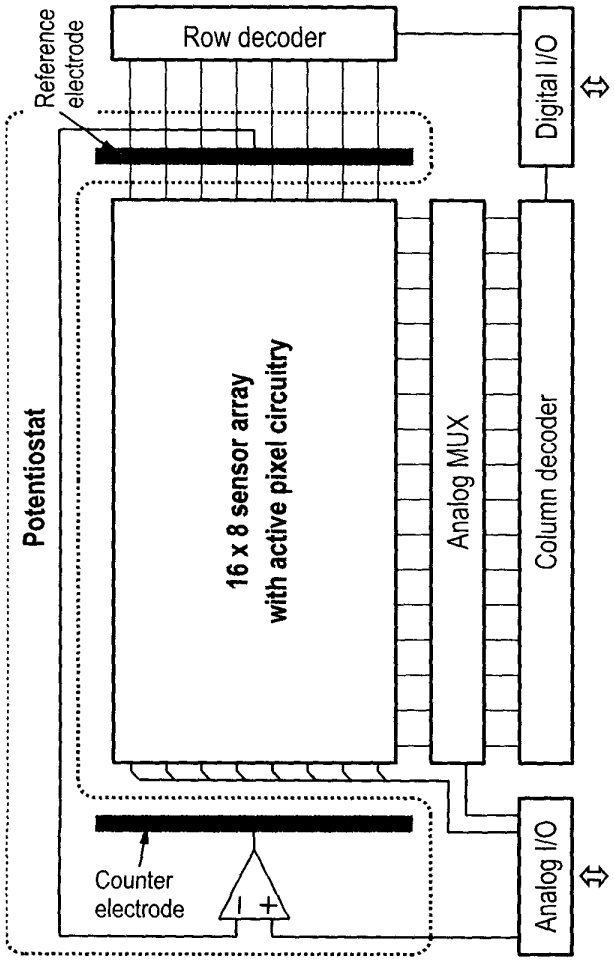

Figure 21.2.6: Chip architecture.

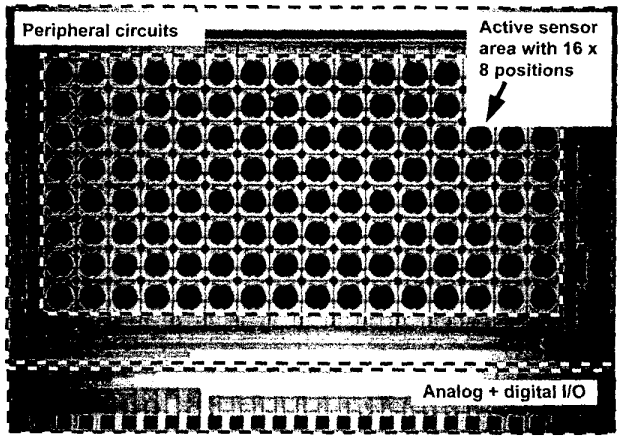

Figure 21.2.7: Chip micrograph of the fabricated active chips.

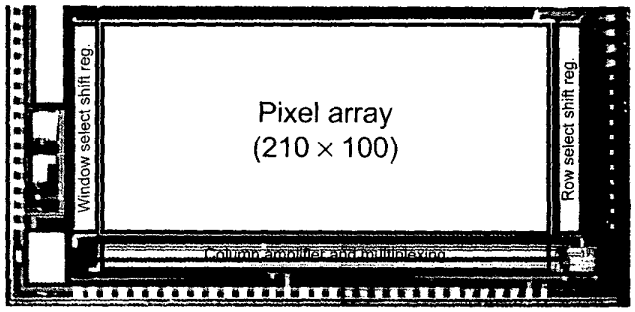

Figure 21.3.7: Chip micrograph.

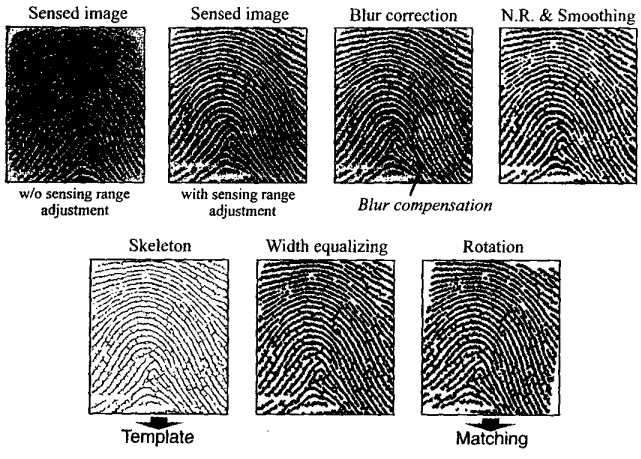

Figure 21.4.7: Results of sensing and image processing.

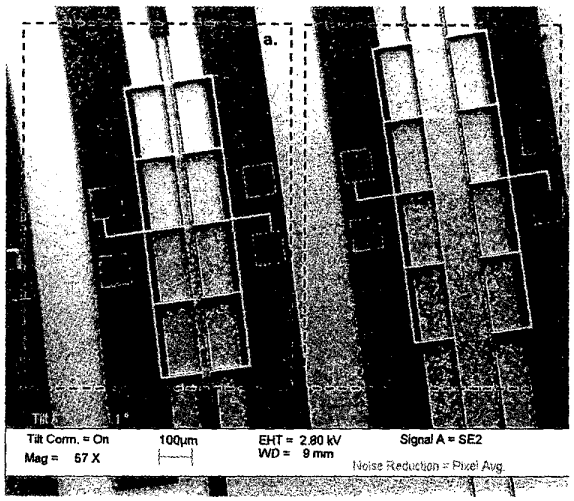

Figure 21.7.7: Die micrograph: (a) 2x2 optoelectronic switch and (b) MZ unbalanced interferometer.